

ANALOG TWO-DIMENSIONAL NETWORK FOR MOTION DETECTION BASED ON LOWER ANIMAL VISION

Kimihiro Nishio, Hiroo Yonezu and Yuzo Furukawa

Department of Electrical and Electronic Engineering, Toyohashi University of Technology

1-1, Hibarigaoka, Tempaku-cho, Toyohashi, Aichi, 441-8580, Japan

Phone : +81-532-44-6747 Fax : +81-532-44-6757

e-mail : nishio@dev.eee.tut.ac.jp

ABSTRACT

A two-dimensional network for motion detection constructed with simple analog circuits was proposed and designed based on the lower animal vision. In the frog visual system, output signals which correspond to the two-dimensional motion direction and velocity are generated by performing simple information processing at the tectum and thalamus. The measured results of the test chip fabricated with 1.2 μ m CMOS process showed that basic circuits utilized in the network can operate correctly. The results with the simulation program with integrated circuit emphasis (SPICE) showed that the network can generate currents which are proportional to the motion direction and the velocity of the object.

Key words : analog integrated circuit, motion detection, retina, tectum, thalamus, vision chip

INTRODUCTION

In biological vision systems, real time image-processing such as motion detection is easily performed since the information processing is accomplished with a hierarchical structure in massively parallel nerve networks. This is difficult in typical image processing systems using Neumann-type computers since the processing is performed in a time-sequential way. The integrated circuit based on biological vision systems can be expected to realize the real-time image processing.

Lower animal visions have the superior function for the motion detection although their brains are simple structures. Therefore, a simple network can be realized based on lower animal visions. Motion detection chips [1],[2] constructed with simple analog circuits have been proposed based on the fly visual system. These chips can perform information processing at a high speed since each unit circuit operates in parallel. However, the structures were limited to one-dimensional array.

Two-dimensional networks for motion detection [3],[4] have been proposed based on the direction selective neuron [5]. One-dimensional motion detection networks were arranged to various directions. The

arranged direction of the one-dimensional network, which outputs the large signal, is the motion direction. However, many one-dimensional networks are needed in order to detect the precise motion direction. This means that the metal wiring is complex in the chip.

The results experimented by Ingle showed that the frog can detect the two-dimensional motion direction and velocity of an object from the signals generated at the tectum and the thalamus [6]. It was clarified that the information processing is equal to that of the model for the simple-shape recognition proposed by Ewert [7]. Since the structure is the rectangular tessellation, the metal wiring is expected to be simple [8]. We proposed the network [9] for simple-shape recognition based on the model [7]. Since the network was the simple, the two-dimensional network for motion detection based on the tectum and thalamus is expected to be simple.

Thus, the proposal and design of the two-dimensional network for motion detection was tried based on the lower animal vision. The measured results of the test chip showed that basic circuits can operate correctly. The results with the simulation program with integrated circuit emphasis (SPICE) showed that the proposed network can detect the motion direction and velocity.

BIOLOGICAL MODEL

An object (spot light) with a constant velocity v is shown in Fig. 1(a). The angle θ_d is the motion direction. The x - and y -component of v are represented by v_x ($=|v_{\text{right}}-v_{\text{left}}|$) and v_y ($=|v_{\text{up}}-v_{\text{down}}|$), respectively.

Figure 1(b) shows a model [6],[7] for detection of the motion direction based on the frog visual system. The left figure is a retina regularly arranged unit cells (a small square) in two-dimensionally. This small square represents a window constructed with photoreceptors. The model in the right figure of Fig. 1(b) is constructed with photoreceptors, tectum type I, thalamus and tectum type II. The signal of the photoreceptor, which is proportional to light intensity, is transmitted to the tectum type I and thalamus. The signals $f_{v,\text{right}}$ and $f_{v,\text{up}}$ are proportional to v_{right} and v_{up} , respectively. The

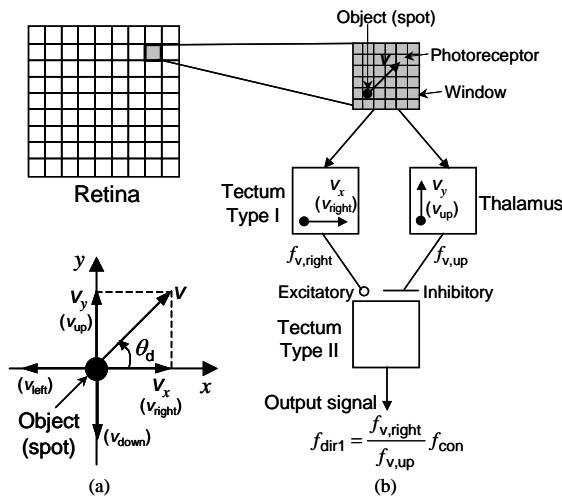


Fig. 1 A model for motion detection based on the frog visual system. (a)The relationship between the object with a constant velocity v and the motion direction θ_d . (b)A model for detection of the motion direction.

tectum type II receives the excitatory signal generated in the tectum type I and the inhibited signal generated in the thalamus. The f_{dir1} is represented by

$$f_{dir1} = \frac{f_{v, right}}{f_{v, up}} f_{con}, \quad (1)$$

where f_{con} is a constant signal. The f_{dir1} becomes f_{con} when the object moves toward $\theta_d = 45^\circ$. The f_{dir1} is approximately proportional to θ_d from 0 to 90° . The θ_d from 0 to 360° can be detected by using four models in Fig. 1(b). The velocity v is given by

$$v = \sqrt{v_x^2 + v_y^2}. \quad (2)$$

Figure 2(a) shows a model for generating signals of v_x and v_y , which is called correlation model [10]. The model is constructed with the unit cell $L_{x,i}$ of the large monopolar cell (LMC), delay neuron $D_{x,i}$ and correlator $C_{x,i}$. Figure 2(b) shows the output signal from each cell when an object (spot) moves toward the right side with the velocity v_x . At first, the output signal $I_{px,1}$ of the photoreceptor is generated when the spot is located in the position $i=1$. The signal $I_{px,1}$ is transmitted to $L_{x,1}$. Then, $L_{x,1}$ generates the constant pulsed signal $V_{Lx,1}$ during the time t_d . The $V_{Lx,1}$ is input to $D_{x,1}$. When the $V_{Lx,1}$ raises, the signal $I_{Dx,1}$ of $D_{x,1}$ indicates the maximum value. After that, the signal of $D_{x,1}$ gradually decreases since the $V_{Lx,1}$ becomes 0. After the time t_v , the spot moves to the position $i=2$. Then, $L_{x,2}$ generates the constant pulsed signal $V_{Lx,2}$. The $I_{Dx,1}$ and $V_{Lx,2}$ are input to $C_{x,1}$. While $V_{Lx,2}$ indicates the constant value, $C_{x,1}$ outputs the signal $I_{Cx,1}$. Then, $I_{Cx,1}$ indicates the peak value $I_{C,peak}$. Since the $I_{C,peak}$ depends on the signal $I_{Dx,1}$, $I_{C,peak}$ is approximately proportional to v_x , which is inversely proportional to t_v . The signal $I_{Cx,2}$ is output from $C_{x,2}$ when the spot moves toward the left side.

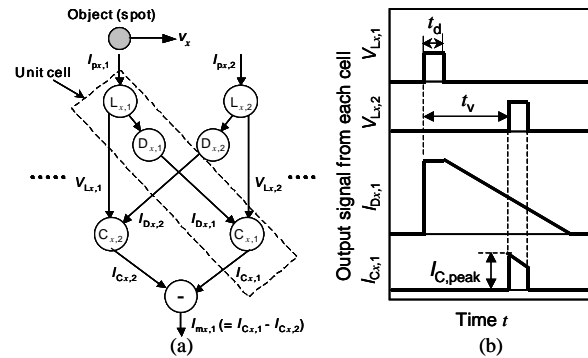


Fig. 2 A model for generating motion signals based on the fly visual system. (a)A model. (b)Output signal from each cell.

The output signal $I_{mx,1}$ is the difference between $I_{Cx,1}$ and $I_{Cx,2}$. The $I_{mx,1}$ shows the positive and negative when the spot moves toward the right side and the left side, respectively. The peak value of the positive $I_{mx,1}$ corresponds to the peak value $f_{v, right}$ in Fig. 1(b), which is proportional to $v_{right} (=v_x)$.

NETWORK FOR MOTION DETECTION

A network based on tectum type I and thalamus

Figure 3 shows a proposed unit network (window) based on tectum type I and thalamus. Since a spot (object) is hardly projected, corner detection circuits (CDC) were inserted to the first stage of the network. The output current $I_{poi,j}$ is a constant current at the corner position. The $I_{poi,j}$ is 0 at the other position. Each $I_{poi,j}$ is summed in x - and y -direction. The current summed in x - and y -direction is $I_{px,i}$ and $I_{py,j}$, respectively. $I_{px,i}$ and $I_{py,j}$ are input to the motion detection circuit (MDC).

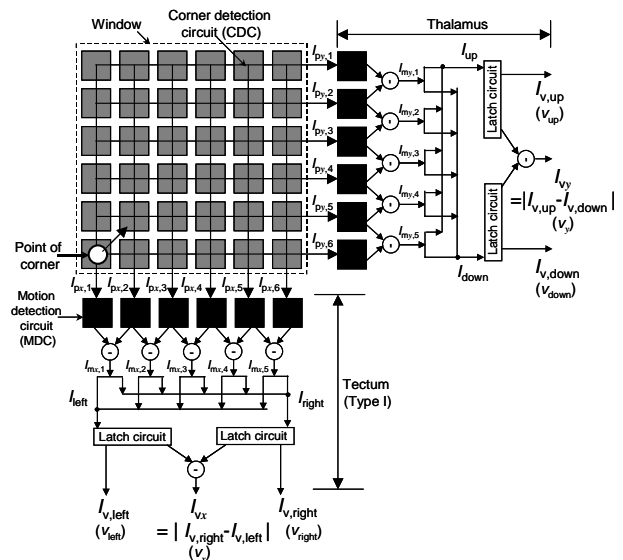


Fig. 3 A unit network for motion detection.

MDC has the function, which is equal to the model in Fig. 2(a). When the corner of the object moves toward the right side and the left side, MDC outputs the pulsed current $I_{mx,i}$ of positive and negative, respectively. The sum of the positive $I_{mx,i}$ is I_{right} . The negative $I_{mx,i}$ is rectified. The sum of the rectified current is I_{left} . Currents I_{up} and I_{down} are obtained when the corner moves toward the upper side and downside, respectively.

It is difficult to perform the signal processing like tectum (type II) since I_{right} and I_{up} are hardly generated at the same time. Thus, each output current of MDC is input to each latch circuit. The output current of the latch circuit, which inputs I_{right} , is $I_{v,right}$. The output current I_{vx} is $|I_{v,right}-I_{v,left}|$. The current I_{vy} is $|I_{v,up}-I_{v,down}|$.

Corner detection circuit (CDC)

Figure 4(a) shows a unit circuit for corner detection (CDC). This circuit is also utilized as an edge detection circuit [11]. Adjacent unit circuits are connected with MN_{r1} and MN_{r2} . Figure 4(b) shows input currents $I_{pi,j}$. The photocurrent $I_{pi,j}$, which is proportional to light intensity, is generated with the photodiode $PD_{i,j}$. $I_{pi,j}$ is input to a smoothing circuit (MN_{r1} and MN_{r2}) and $I_{hi,j}$ is generated. At the corner positions, $I_{pi,j}$ is diffused in two directions. At the edge positions, $I_{pi,j}$ is diffused in the only one direction. Thus, $I_{hi,j}$ at the corner positions are smaller than that at the edge positions. The circuit outputs $I_{bi,j}$ which is the difference between $I_{pi,j}$ and $I_{hi,j}$. The absolute value of $I_{bi,j}$ at the nearest corner position is larger than that at the other positions. The I_{th1} is a threshold current. The output voltage $V_{bi,j}$ is the supply voltage V_{DD} in the condition of $I_{pi,j} \gg I_{hi,j} + I_{th1}$, which means the corner position. Then, the output current $I_{poi,j}$ is a constant current I_{con1} since MN_{po1} turns on.

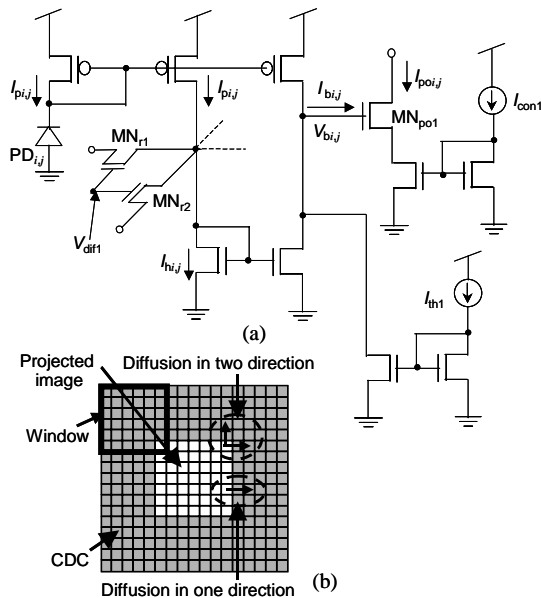


Fig. 4 A corner detection circuit (CDC). (a)A unit circuit. (b)Photocurrents (Input image).

Motion detection circuit (MDC) and latch circuit

A motion detection circuit (MDC) is shown in Fig. 5(a). When the corner is located in the circuit, the input current $I_{px,1}$ is larger a threshold current I_{th2} . Then, MN_{M1} turns on since the voltage V_2 becomes V_{DD} . Since the voltage V_1 becomes V_{DD} after the time t_d by a capacitor C_P , MP_{M1} turns on during the time t_d . Then, a constant current I_{con2} flows into MP_{M2} . I_{th3} becomes smaller value than I_{con2} by designing the larger channel length of MN_{M3} than that of MN_{M2} . $V_{Lx,1}$ becomes V_{DD} during t_d . Since MN_{D1} turns on, $V_{Dx,1}$ shows a constant voltage by a constant current I_{con3} . After the time t_d , MN_{D1} turns off since $V_{Lx,1}$ becomes 0. Since $V_{Dx,1}$

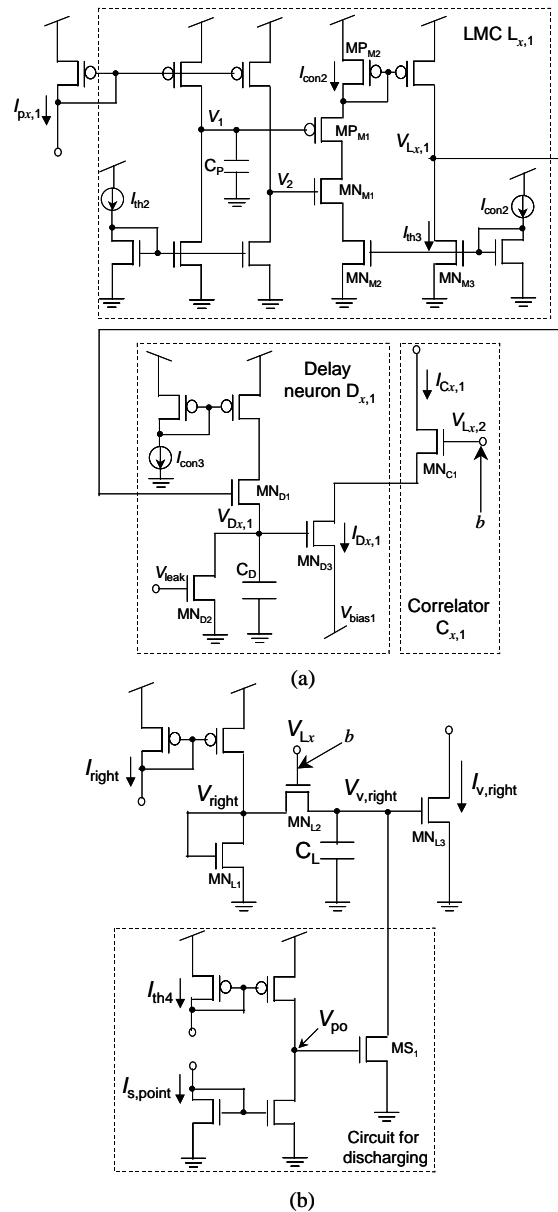


Fig. 5 A motion detection circuit (MDC) based on the correlation model and a latch circuit. (a)A motion detection circuit. (b)A latch circuit.

gradually decreases by MN_{D2} , the current $I_{Dx,1}$ also decreases. $V_{Lx,2}$ is V_{DD} when the corner moves to the adjacent unit circuit of the right side. Then, $I_{Cx,1}$ is equal to $I_{Dx,1}$ since MN_{C1} turns on.

The latch circuit is shown in Fig. 5(b). The pulsed current I_{right} is converted to the voltage V_{right} . The gate of the MN_{L2} is connected to the node b in Fig. 5(a). When I_{right} shows the pulse ($I_{Cx,1}=I_{Dx,1}$), MN_{L2} turns on since V_{Lx} is V_{DD} . Then, $V_{v,right}$ is nearly equal to V_{right} . The $V_{v,right}$ is converted to the current $I_{v,right}$ by MN_{L3} . $I_{v,right}$ becomes nearly equal to I_{right} . After that, V_{Lx} becomes 0 and MN_{L2} turns off. Then, $V_{v,right}$ is latched by the capacitor C_L . The circuit for discharging when the corner is not located in the window is inserted. The circuit inputs the current $I_{s,point}$ and the threshold current I_{th4} . The sum of output currents $I_{poi,j}$ of CDC is $I_{s,point}$. I_{th4} is set to the smaller value than I_{con1} in Fig. 4(a). When the corner is not located in the window, the voltage V_{po} is V_{DD} . Then, MS_1 turns on. Since $V_{v,right}$ becomes 0, $I_{v,right}$ also gets close to 0.

Circuit for detection of motion direction (CDMD) and velocity detection circuit (VDC)

A circuit for detection of motion direction (CDMD) based on tectum type II is shown in Fig. 6(a). The output current I_{dir1} is given by a following equation [12],

$$I_{dir1} \cong \frac{I_{v,right}}{I_{v,up}} I_{con4}, \quad (3)$$

where I_{con4} is a constant current. The θ_d from 0 to 90° can be detected from I_{dir1} . Thus, the θ_d from 0 to 360° can be detected by using four circuits in Fig. 6(a).

A velocity detection circuit (VDC) based on eq. (2) is shown in Fig. 6(b). This circuit is constructed with two square circuits and a square root circuit [13]. The square circuit and the circuit in Fig. 6(a) are same structures. Output currents of square root circuits which input I_{vx} and I_{vy} are I_x and I_y , respectively. The sum of I_x and I_y is I_{sum} . I_{sum} is input to the square root circuit. The output current I_{vel} is given by

$$I_{vel} \cong (I_0 I_{sum} \exp(V_{bs}))^{1/2} \propto \sqrt{I_{vx}^2 + I_{vy}^2}, \quad (4)$$

where I_0 and V_{bs} are a leak current and a constant voltage, respectively. I_{vel} is proportional to the velocity v in (2).

EXPERIMENTAL AND SIMULATION RESULTS

Measured results of basic circuits

A test chip of basic circuits was fabricated with $1.2\mu\text{m}$ CMOS process. The photograph of the test chip is shown in Fig. 7(a). Twenty CDC and MDC are arranged to one-dimensionally. Capacitors C_p and C_D were fabricated with 1pF. The area of the unit circuit constructed with CDC and MDC was $55 \times 215 \mu\text{m}^2$ (PD:

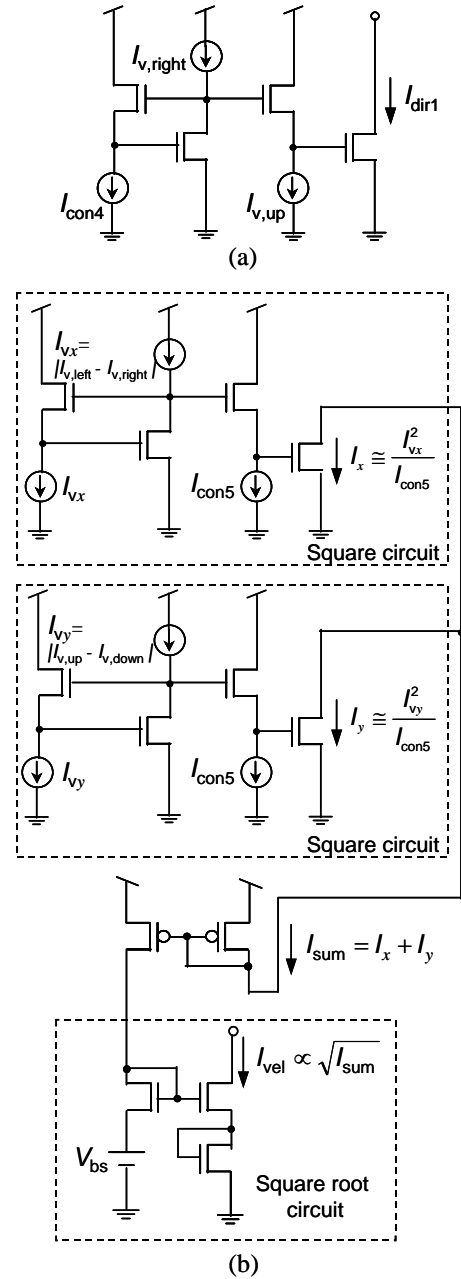


Fig. 6 Circuit for detection of motion direction (CDMD) and velocity detection circuit (VDC). (a)CDMD. (b)VDC.

$50 \times 50 \mu\text{m}^2$). The CDMD and the square root circuit in Fig. 6(b) were fabricated with the same process in another chip. In all measurements, V_{DD} was set to 3V.

The measuring equipment is shown in Fig. 7(b). An image generated by PC was irradiated from a projector. The image was projected on the chip through a lens. Photocurrents were about 50nA and 100pA when white and black images were projected on PD, respectively.

MDC with CDC of $i=9$ was measured. V_{dif1} , I_{th1} and I_{con1} were set to 1.58V, 6nA and 5nA, respectively. I_{th2} , I_{con2} , I_{con3} , V_{leak} and V_{bias1} were set to 3nA, 5nA, 100nA,

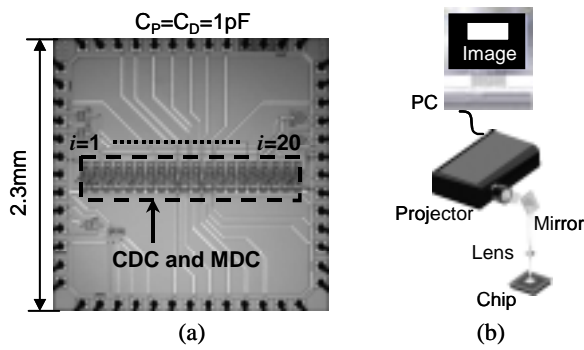


Fig. 7 A photograph of the test chip and a measuring equipment. (a)A photograph of the chip. (b)A measuring equipment.

0.45V and 1.0V, respectively. The relationship between the corner and PD is shown in Fig. 8(a). The edge position is equal to the corner position since the network is arranged to one-dimensionally. The time for passing through L_p+L_a is t_v in Fig. 2(b). An object (white image) moved toward the right side (from $i=1$ to $i=20$).

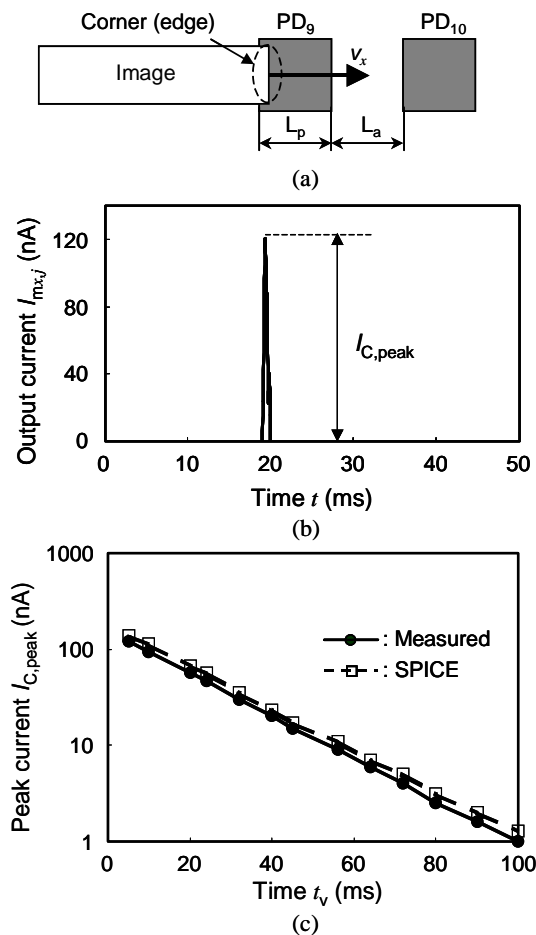


Fig. 8 The measured results and the simulation results of the MDC with CDC. (a)The relationship between the object with velocity v_x and PD. (b)Output current $I_{mx,i}$ at $i=9$ obtained by measuring the test chip. (c)The relationship between the peak current $I_{C,peak}$ and the time t_v .

Figure 8(b) shows the output current $I_{mx,i}$ of MDC at $i=9$. MDC at $i=9$ generated the positive $I_{mx,i}$ when the corner moved to PD at $i=10$. The maximum value of the pulse is $I_{C,peak}$. The relationship between $I_{C,peak}$ and t_v is shown in Fig. 8(c). It was clarified that $I_{C,peak}$ is approximately proportional to v_x , which is inversely proportional to t_v . It was confirmed that the $I_{mx,i}$ shows the negative when the object moves toward the left side.

Figure 9(a) shows the output current I_{dir1} of CDMD. The input current $I_{v,right}$ was changed from 0 to 10nA. When I_{con4} and $I_{v,up}$ were set to 10nA, I_{dir1} became $I_{v,right}$. When I_{con4} and $I_{v,up}$ were respectively set to 5nA and 10nA, I_{dir1} became the half value of $I_{v,right}$. Thus, the output current I_{dir1} corresponded to that in (7).

The output current I_{vel} of the square root circuit is shown in Fig. 9(b). The voltage V_{bs} was set to 0.61V. The input current I_{sum} was changed from 0 to 100nA. When I_{sum} was 100nA, I_{vel} showed about 10nA ($=\sqrt{100}$ nA). It was clarified that the circuit operates normally.

Measured results in Figs. 8 and 9 were approximately equal to simulation results with SPICE.

Simulation results of two-dimensional network

The network arranged unit networks in Fig. 3 to two-dimensionally was simulated with SPICE. The network was constructed with 42×42 CDC. Since the unit network was constructed with 6×6 CDC,

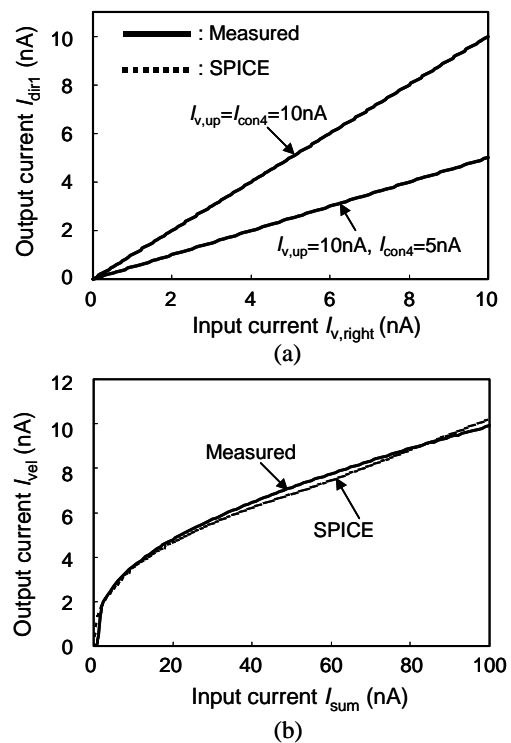


Fig. 9 The measured results and the simulation results of CDMD and the square root circuit. (a)Output current I_{dir1} of CDMD. (b)Output current I_{vel} of the square root circuit.

7×7 windows were arranged to two-dimensionally. The capacitor C_L was set to 0.5pF . I_{th4} , I_{con4} and I_{con5} were set to 3nA , 10nA and 100nA , respectively

The input image is shown in Fig. 10(a). A white square projected on 13×13 PD is an object. The object moved toward $\theta_d = 45^\circ$ as reducing the speed. Figure 10(b) shows the output current I_{vel} , which is displayed with the image of 7×7 array. In dependence on the speed reduction of the object, I_{vel} was displayed with close color in the black. Thus, it was clarified that the velocity can be detected by using I_{vel} .

The same network was simulated in the condition that the object changing the motion direction with a constant velocity was projected. The input image is shown in Fig. 11(a). Figure 11(b) shows the output current I_{dir1} . In dependence on the increase of θ_d , I_{dir1} was displayed with close color in the black. Thus, it was clarified that the motion direction can be detected by using I_{dir1} .

The power consumption of each circuit was evaluated with SPICE. The results are shown in Table 1. All maximum powers were smaller values than $1\mu\text{W}$.

Table 1 Maximum power consumption of each unit circuit.

	CDC	MDC	Latch	CDMD	VDC
Max power (μW)	0.68	0.66	0.76	0.46	0.86

DISCUSSION

A two-dimensional network for motion detection constructed with simple analog circuits was proposed based on the lower animal vision. Basic circuits were characterized by low-power consumption, since the circuits operate in a subthreshold region.

The measured results of basic circuits were good agreement with simulation results, as shown in Figs. 8(c) and 9. Thus, we can believe to fabricate a chip which contains a large number of unit circuits.

The proposed network could detect the more precise direction as compared with previous proposed networks [3],[4]. It was clarified from the results in Fig. 11(b) that at least 20 directions can be detected by using four circuits in Fig. 6(a).

In this study, the simple shape (square) was only projected. Corner detection circuits (CDC) and edge detection circuits are same structure [11]. We clarified that the circuits can detect edge positions when the object of the complex shape is projected [11]. Thus, CDC can detect corner positions even if the object of the complex shape is projected.

The model in Fig. 1 generated signals of the motion direction and velocity. The model proposed by Ewert can generate signals of the simple-shape from each window. We proposed the network [9] for recognizing the simple shape such as a circle, square and triangle based on the model. It is able to generate signals of the direction, velocity and simple shape by inserting the network for recognizing the simple shape to the proposed network. Frogs can discriminate a food from an enemy with a complex shape by sensing the motion and shape. Similarly, the proposed network can discriminate objects such as a car, a person and a ball by aggregating signals of the motion direction, velocity and simple shape. It was reported that the tectum in the frog brain corresponds to the superior colliculus in the vertebrate brain, which generates signals for target tracking [14]. By using the proposed network, it is possible to discriminate the object and the track the selected object. The signals of the motion direction and velocity are utilized as signals of the motor control for the target tracking. Thus, the application of the network can be expected to advance the chip for the target tracking.

We have proposed the network [9] for detection of object approach based on the locust visual system. It is easy to connect the proposed network with the network for approach detection since these structures are same.

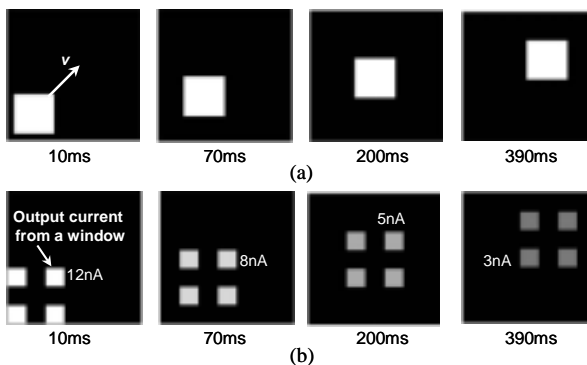


Fig. 10 Simulation results of the two-dimensional motion detection network. (a)Input image. (c)Output current I_{vel} .

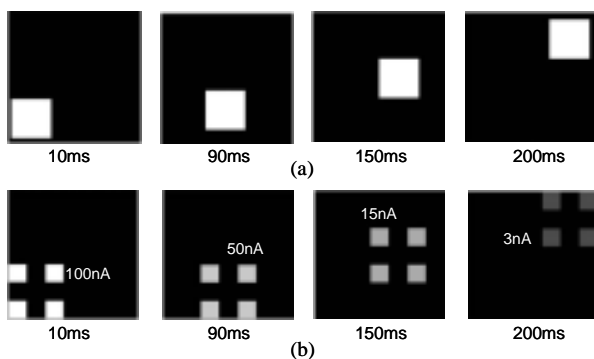


Fig. 11 Simulation results of the two-dimensional motion detection network. (a)Input image. (c)Output current I_{dir1} .

The application of the connected network can be realized the three-dimensional motion detection.

CONCLUSION

A two-dimensional network for motion detection was proposed and designed based on the lower animal vision. The network was constructed with simple analog circuits. The measured results of the test chip fabricated with 1.2 μ m CMOS process showed that the basic circuits constructed with the network can operate correctly. It was apparent from the simulation results that the proposed network can detect the motion direction and the velocity of the object. Thus, the integrated circuit for the two-dimensional motion detection can be realized by using the proposed network. The application of the network is expected to advance tracking systems and to realize the three-dimensional motion detection.

ACKNOWLEDGEMENT

The work was supported in part by the Ministry of Education, Science, Sports and Culture under a Grant-in-Aid for Scientific Research. It was also supported by the 21st Century COE Program "Intelligent Human Sensing", under the same Ministry, and partially supported by the Toyohashi University of Technology Venture Business Laboratory (TUT-VBL). The VLSI chip in this study has been fabricated in the chip fabrication program of the VLSI Design and Education Center (VDEC), the University of Tokyo in collaboration with On-Semiconductor, Nippon Motorola LTD., HOYA Corporation, and KYOCERA Corporation.

REFERENCES

- [1] M. Ohtani, H. Yonezu and T. Asai, "Analog Metal-Oxide-Silicon IC Implementation of Motion-Detection Network Based on Biological Correlation Model", *Jpn. J. Appl. Phys.*, vol.39, pp.1160-1164, 2000.
- [2] S. C. Liu, "A Neuromorphic a VLSI Model of Global Motion Processing in the Fly", *IEEE Trans. on Circuits and Systems II*, vol. 47, pp. 1458-1467, 2000.
- [3] M. Ohtani, H. Yamada, K. Nishio, H. Yonezu and Y. Furukawa, "Analog LSI Implementation of Biological Direction-Selective Neuron", *Jpn. J. Appl. Phys.*, vol. 41, pp. 1409-1416, 2002.
- [4] K. Boahen, "Retinomorphich Chips that see Quadruple Images", *Proceedings of Micro Neuro '99*, 1999.
- [5] J. K. Douglass and N. J. Strausfeld, "Visual Motion-Detection Circuits in Flies : Parallel Direction- and Non-Direction-Sensitive Pathways between the Medulla and Lobula Plate", *J. Neuroscience*, pp. 4551-4562, 1996.
- [6] D. Ingle, "Two Visual Systems in the Frog", *Science*, vol. 181, pp. 1053-1055, 1973.
- [7] A. P. Ewert, "The Neural Basis of Visually Guided Behavior", *Scientific American*, vol. 240, pp. 34-42, 1974.
- [8] A. Moini, *Vision Chips*, Kluwer Academic Publishers, 1999.
- [9] K. Nishio, H. Yonezu, M. Ohtani, H. Yamada and Y. Furukawa, "Analog Metal-Oxide-Semiconductor Integrated Circuit Implementation of Approach Detection with Simple-Shape Recognition Based on Visual Systems of Lower Animals", *Optical Review*, vol.10, pp. 96-105, 2003.
- [10] W. Reichardt, *Principles of Sensory Communication*, Wiley, New York, 1961.
- [11] H. Yamada, T. Miyashita, M. Ohtani, K. Nishio, H. Yonezu and Y. Furukawa, "An Integrated Circuit for Two-Dimensional Edge-Detection with Local Adaptation Based on Retinal Networks", *Optical Review*, vol. 9, pp.1-8, 2002.
- [12] A. G. Andreou, K. A. Boahen, P. O. Pouliquen, A. Pavasovic, R. E. Jenkins and K. Strohhahn, "Current-Mode Subthreshold MOS Circuits for Analog VLSI Neural Systems", *IEEE Trans. Neural Networks*, vol.2, pp. 205-213, 1991.
- [13] C. A. Mead, *Analog VLSI and Neural Systems*, Addison Wesley, New York, 1989.
- [14] R. L. Didday, "A Model of Visuomotor Mechanism in the Frog Optic Tectum", *Mathematical Biosciences*, vol. 30, pp. 169-180, 1976.